Master of Science

The Functional Study of S100A11 in Triple Negative Breast Cancer

The Graduate School

of the University of Ulsan

Department of Medical Sciences

Dong-Hee Kang

The Functional Study of S100A11 in Triple Negative Breast Cancer

Supervisor: Dong-Hoon Jin

A Dissertation

Submitted to

the Graduate School of the University of Ulsan

In partial Fulfillment of the Requirements

for the Degree of

Master of Science

by

Dong-Hee Kang

Department of Medical Science

University of Ulsan, Korea

August 2024

The Functional Study of S100A11 in Triple Negative Breast Cancer

This certifies that the dissertation of Dong-Hee Kang is approved

_____

Committee Chair Dr. Chang Hoon Ha

_____

Committee Member Dr. In Ki Kim

_____

Committee Member Dr. Dong-Hoon Jin

Department of Medical Science

University of Ulsan, Korea

August 2024

ABSTRACT

Triple negative breast cancer (TNBC) is the most aggressive subtype of this disease, accounting for approximately 15% of all breast cancers. Moreover, the prognosis of patients with this subtype is exacerbated by its high metastasis and recurrence rates, as well as drug resistance. However, treatments are limited owing to a lack of suitable receptors to target. In this study, I performed transcriptome profiling for breast cancer and TNBC based on reference to the Gene Expression Omnibus (GEO) database. I found evidence to indicate that S100 calcium-binding protein A11 (*S100A11*) is a potential therapeutic target. S100A11 is an S100A protein that regulates enzyme activity and several cellular mechanisms in response to calcium ions. Although S100A11 has been extensively studied in the field of cancer research as a tumor-promoting factor, there has to date been no research conducted on this protein in the context of breast cancer. During the course of this study, I validated the functionality of *S100A11* based on analyses of *in silico* data, patient samples, and breast cancer cell lines. Data retrieved from the TCGA database revealed S100A11 to be highly expressed in patients with breast cancer. Analysis of patient samples indicated that, compared with normal tissues, S100A11 expression is upregulated in cancer tissues depending on the grade, and that expression patterns are also associated with patient prognosis. Inhibition of S100A11 was found to promote a significant increase in cell death, particularly in TNBC cell lines. Furthermore, the findings of western blot and RT-qPCR analyses revealed a correlation between the expression of S100A11 and that of BIM. Moreover, S100A11 knockdown-mediated AKT-FoxO3a signaling was found to activate BIM expression, and thereby induce apoptosis. On the basis of this elucidation of the mechanisms whereby S100A11 functions in TNBC, I propose S100A11 to be a novel biomarker and new therapeutic target for the treatment of TNBC.

Keywords: S100A11, Triple negative breast cancer, Apoptosis, Biomarker, Therapeutic target, BIM, FoxO3a

CONTENTS

LIST OF FIGURES

LIST OF TABLES

INTRODUCTION

Breast cancer, a disease characterized by considerable heterogeneity hindering treatment effectiveness, has emerged as the most frequently diagnosed major malignancy worldwide [1, 2]. One in six women develop breast cancer, and it is the leading cause of cancer-related death in women [3]. In addition, in recent years, the incidence of breast cancer among men has increased [4]. Moreover, given the increasing obesity incidence and the older adult population, the prevalence and mortality rates of breast cancer are anticipated to increase further in the near future [5]. Breast cancer can occur as a range of different subtypes, for which estrogen receptor (ER), progesterone receptor (PR), and human epidermal growth factor receptor 2 (HER2) have been identified as diagnostic pathological indicators. Among the different subtypes, ER-positive tumors account for more than 70% of breast cancers and are associated with a slow progression of the disease, whereas ER-negative tumors are hormone-independent and are characterized by a more aggressive behavior. In contrast, PR, induced by estrogen, is considered a favorable prognostic marker, whereas HER2, the most well-established prognostic factor in the epidermal growth factor receptor family, tends to be indicative of poor survival when amplified or overexpressed [6, 7].

Triple negative breast cancer (TNBC) refers to a type of breast cancer that is negative for ER, PR, and HER2 [8]. Patients with TNBC are mainly premenopausal women below 40 years of age, and they account for approximately 15–20% of patients with breast cancer. Notably, the survival of patients diagnosed with TNBC is shorter than that of patients with other breast cancer subtypes, with a mortality rate of up to 40% within the first 5 years post-diagnosis. TNBC is highly invasive, with approximately 46% of patients developing distant metastases, after which the average survival time is only 13 months. Furthermore, whereas the average recurrence period for patients without TNBC is between 35 and 67 months, that for patients with TNBC is only 19 to 40 months, and the mortality rate within 3 months after recurrence reaches 75% [9, 10].

Proteins in the S100 family are widely distributed in vertebrates, in which they are the largest subgroup of Ca^{2+}-binding EF-hand proteins, characterized by a helix E-loop-helix F structure [11, 12]. The S100 family comprises approximately 25 proteins, including 16 S100A proteins (S100A1 to S100A16) located on chromosome 1q21 and additional members such as S100B, S100G, S100P, and S100Z located on other chromosomes [13, 14]. However, despite the considerable sequence and structural similarities within members of the S100 family, functional interchangeability is limited. These proteins have been established to play diverse roles in biological processes, including cell proliferation, migration, invasion, inflammation, and differentiation [15–19].

Among these S100 proteins, S100 Calcium Binding Protein A11 (*S100A11*) is a gene corresponding

to the S100A protein. In the presence of calcium ions in cells, this protein regulates enzyme activity by inhibiting ATPase activity or is phosphorylated and enters the nuclear to regulate cell growth. S100A has also been established to be involved in the cell cycle, growth, survival, and apoptosis, and is generally distributed in both the nucleus and cytoplasm [20]. Recently, the function of S100A11 in cancer has been widely reported, being identified as a tumor suppressor gene in bladder cancer [21], but is also known as a tumor-promoting gene in colon cancer [22, 23], stomach cancer [24, 25], hepatocellular carcinoma [26], lung cancer [27], ovarian cancer [28], pancreatic cancer [29, 30], prostate cancer [31], and kidney cancer [32]. However, despite this broad characterization, there remain numerous cancer types in which S100A11 yet to be studied, among which, its function in breast cancer has not been established yet.

In this study, I established the molecular mechanisms underlying the action of S100A11 in breast cancer. S100A11 demonstrated high expression in tissues from patients with breast cancer. Moreover, S100A11 knockdown can induce apoptosis by activating BIM mediated through the AKT/FoxO3a pathway in TNBC. Based on these findings, S100A11 may have potential utility as a novel therapeutic target for TNBC.

MATERIAL & METHODS

1. GEO database analysis

The Gene Expression Omnibus Database (GEO) serves as a public functional genomics data repository that accepts MIAME-compliant submissions of gene expression data, microarray data, and gene chips.

In this study, I utilized the genomic expression data set of GSE32641. The GSE32641 database includes 90 tumor tissues and 7 normal tissues from patients with breast cancer. Using this, I analyzed genes differentially expressed between tumors and normal tissues. Significant differentially expressed genes (DEGs) were detected using adjusted P-value and Benjamini-Hochberg false discovery rate. Upregulated genes were identified using cutoff values of $P < 0.001$ and logFC > 2.0

2. Gene expression boxplot and OS analysis

Overall survival (OS) charts were examined to evaluate the prognosis of patients according to the level of S100A11 expression. I also established boxplot expression analysis to evaluate S100A11 expression levels in both normal and tumor specimens. The analysis was performed using GEPIA2 (http://gepia.cancer-pku.cn/), a well-established and widely used tool for gene expression analysis utilizing tumor and normal sample datasets [33].

3. Specimens and Cell culture

A total of 12 breast cancer tissues were used in this study. The breast cancer tissues were obtained from the Biological Resource Center (BRC) of Asan Medical Center in Seoul.

HCC-1395, HCC-1937, HCC-1954, MCF-7, MDA-MB-231, SK-BR-3, and T47D cell lines were all purchased from Korea Cell Line Bank (KCLB, Seoul, Korea). HCC-1395 cells were cultured in RPMI-1640 medium (WELGENE, Daegu, Korea) supplemented with 25mM HEPES (WELGENE), 100 mg/ml penicillin-streptomycin (WELGENE), and 10% Fetal Bovine Serum (FBS, GIBCO, New York, USA). HCC-1937, HCC-1954, MCF-7, MDA-MB-231, and T47D cells were cultured in RPMI-1640 medium (WELGENE) supplemented with 100 mg/ml penicillin-streptomycin (WELGENE), and 10% FBS (GIBCO). SK-BR-3 cells were cultured in McCoy's 5A (Modified) Medium (GIBCO) containing 100 mg/ml penicillin-streptomycin (WELGENE) and 10% Fetal Bovine Serum (GIBCO). Cells were maintained in an incubator with 5% CO_2 and maintained at 37°C.

4. Transfection

Cells were transiently transfected with the target siRNA using jetPRIME® Transfection reagent (Polyplus, Illkirch, France) following the manufacturer's instructions. S100A11 and BIM targeting siRNAs, shRNAs, and negative control siRNAs were obtained from GENOLUTION (Seoul, Korea). The sequences of siRNA and shRNA against S100A11 and BIM used in this study are as follows: siS100A11: 5'-GUG UCC UUG ACC GCA UGA UTT-3'; shBIM: 5'-GAC CGA GAA GGU AGA CAA UUG UCU CCA AUU GUC UAC CUU CUC GGU CUU-3'.

5. Trypan blue exclusion assay

HCC-1395, HCC-1937, HCC-1954, MCF-7, MDA-MB-231, SK-BR-3, and T47D cells were plated on 60 mm plates at 40% density after 24 hours. Then, cells were transfected with siRNAs and harvested after 12-72 hours. Cells were collected, suspended in 1X Phosphate-buffered saline (PBS), and stained with 0.4% trypan blue staining solution (GIBCO). A total of 20 microliters of the mixture was placed on a hemocytometer (Marienfeld-Superior, Lauda-Königshofen, Germany) and analyzed using a light microscope (Olympus, Tokyo, Japan). Both live (unstained) and dead (stained) cells in the hemocytometer were counted according to the manufacturer's instructions. The total cell number was counted. Triplicate measurements were performed for each sample.

6. Annexin V/PI staining assay

Cells (1.5×10^5 cells/well) were seeded in 60 mm cell culture dishes (SPL Life Sciences, Pocheon-si, Korea) and transfected with siRNA 24 hours later. After culturing in an incubator for 72 hours, cells were harvested using 1X Trypsin-EDTA (WELGENE). After washing with 1X PBS and resuspending the cells in 1X Binding buffer, they were stained with FITC Annexin V Apoptosis Detection Kit I (556547, BD Biosciences, New Jersey, USA). Afterwards, they were stained for 15 minutes at room temperature (RT) protected from light and analyzed by flow cytometry (BD Biosciences, San Jose, CA, USA).

7. Cell cycle analysis

Cells (1.5×10^5 cells/well) were seeded in 60 mm cell culture dishes (SPL Life Sciences) and transfected using siRNA 24 hours later. After incubation for 72 hours, cells were harvested using 1X Trypsin-EDTA (WELGENE). The cells were washed with 1X PBS, then Methyl Alcohol (DUKSAN,

Ansan-si, Korea) was added and the cells were fixed at -20°C for 24 hours. The cells were washed, mixed with 1X PBS, RNase (100 μg/ml, Roche, Basel, Switzerland), and Propidium Iodide Staining Solution (50 μg/ml, BD Biosciences), then blocked from light and allowed to rest for 10 minutes at RT. They were then analyzed by flow cytometry (BD Biosciences).

8. TUNEL assay

Cells (1×10^5 cells/well) were seeded in confocal dishes (SPL Life Sciences) and transfected with siS100A11 24 hours later. After 48 hours, the culture medium was removed, 4% paraformaldehyde (Biosesang, Yongin-si, Korea) was added, and the cells were rest on ice for 1 hour. After removing 4% paraformaldehyde and washing with 1X PBS, 0.2% Triton X-100 was added and incubated at 37°C for 10 minutes. After removing 0.2% Triton X-100, the following steps were performed using the One-step TUNEL In Situ Apoptosis Kit (Green, FITC) (E-CK-A320, Elabscience, Texas, USA) according to the manufacturer's instructions. After all steps were completed, the cells were washed with 1X PBS, the moisture was completely removed, and the stained cells were examined by confocal analysis.

9. Quantitative real-time PCR

Total RNA was extracted using TRIzol® (Invitrogen, California, USA). cDNA was synthesized by reverse transcription of 1 μg of total RNA using AccuPower® RT PreMix (Bioneer, Daejeon, Korea). Quantitative real-time PCR was performed using SYBR™ Select Master Mix (Applied Biosystems, Boston, USA) according to the manufacturer's instructions. As a positive control, *GAPDH*, a housekeeping gene to standardize the variability of expression level, was used as an internal control, and as a negative control, only distilled water, primer, and SYBR Green were included. The sequences of primers used in this experiment are listed in Table 1, and each experiment was performed independently three times.

10. Reverse transcription-PCR

RNA was extracted using TRIzol® (Invitrogen) and 1 μg of total RNA was synthesized into cDNA using AccuPower® RT PreMix (Bioneer). PCR reactions began with a pre-denaturation step of 5 minutes at 95°C, followed by 30 cycles of denaturation at 95°C for 30 seconds, primer annealing at 54°C for 25 seconds, and primer extension at 72°C for 30 seconds. Once the cycling step was complete, a final extension was made for 5 minutes at 72°C. And the same primers as quantitative real-time PCR were used (Table 1). Bands were identified by electrophoresis using agarose gels (Lonza, Basel,

Switzerland) diluted to 2% in 1X Tris-borate-EDTA buffer (TBE buffer; T&I, Kangwon, Korea). *GAPDH* mRNA was used as a loading control.

11. Subcellular fractionation

Cells (1×10^5 cells/well) were processed using the Intracellular Protein Fractionation Kit for Cultured Cells (78840, Thermo Fisher Scientific, Massachusetts, USA) according to the manufacturer's instructions. cytosol extraction buffer (CEB) containing 1X phosphatase inhibitor cocktail was added to the washed cells and mixed for 10 minutes at 4°C. Then centrifugation at 500 g at 4°C for 5 minutes was performed. After collecting the supernatant from which the cytosol was extracted, membrane extraction buffer (MEB) containing 1X phosphatase inhibitor cocktail was added to the cell pellet and mixed for 10 minutes at 4°C. Then centrifugation at 3000 g at 4°C for 5 minutes was performed. After discarding the supernatant, nuclear extraction buffer (NEB) containing 1X phosphatase inhibitor cocktail was added to the cell pellet and mixed for 30 minutes at 4°C. Finally, the supernatant containing the extracted nucleus was collected by centrifugation at 5000 g at 4°C for 5 minutes.

12. Western blot assay

Cells were added to Radioimmunoprecipitation assay buffer (RIPA buffer; T&I) containing protease and phosphatase inhibitor cocktail (Roche) and then lysed for 30 minutes on ice. The supernatant was collected by centrifugation at 13,000 rpm for 20 minutes at 4°C, and the concentration of the extracted protein was measured using the bradford assay (Bio-Rad, Hercules, CA, USA). After quantifying the protein at a certain concentration, it was mixed with 5X loading dye (T&I) and heated to 100°C. The samples were then separated using Sodium dodecyl-sulfate polyacrylamide gel electrophoresis (SDS-PAGE) and transferred to Polyvinylidene difluoride (PVDF; Millipore, Boston, USA) membrane. To block non-specific bands other than the target, the band was blocked with 5% skim milk and left overnight at 4°C to attach antibodies. Information on the antibodies used in this experiment is listed in Table 2. Then, the membrane was incubated with secondary antibodies (Santa Cruz Biotechnology, CA, USA) for 1 hour at RT. After simple washing with 1X Tris-Buffered Saline with Tween 20 (TBS-T; T&I), protein bands were detected using chemiluminescence western blotting detection kit (Amersham, Little Chalfont, Buckinghamshire, UK).

13. Immunofluorescence

Cells (1×10^5 cells/well) were seeded in confocal dishes (SPL Life Sciences) and transfected 24

hours later. The medium was removed 12 hours later and the cells were washed using 1X PBS. After fixing the cells at 37°C for 10 minutes using 4% paraformaldehyde (Biosesang), the solution was removed and the cells were washed using 1X PBS. 0.1% Triton X-100 diluted in 1X PBS was added to the cells and incubated for 15 minutes at RT. The solution was removed and the cells were washed thoroughly using 1X PBS. Prepare 2% BSA using 1X PBS, add to cells and incubate for 1 hour at RT. The solution was removed and the antibodies (Table 3) were diluted in 0.1% BSA and incubated overnight at 4°C. After removing the primary antibody solution and washing the cells with 1X PBS, secondary antibodies (Invitrogen) diluted in 0.1% BSA labeled with a fluorescent dye were added and incubated for 1 hour at RT, blocking light. After washing the cells with 1X PBS with Tween 20, they were mounted with a Antifade Mounting Medium with DAPI (H-1200-10; Vector Laboratories, California, USA). Detection was confirmed using a fluorescence microscope (ZEISS, LSM710, Baden-Württemberg, Germany), and the images were analyzed using ZEN software (Carl Zeiss Co. Ltd, Seoul, Korea).

14. Immunohistochemistry

Breast cancer and normal Tissue Microarray (BR483) was purchased from TissueArray.Com LLC (Derwood, USA). Place the paraffin slide in a 60°C oven and incubate for 1 hour to melt the paraffin wax. After cooling the slide, immerse it in xylene (DUKSAN) three times for 5 minutes each, followed by 100% ethanol twice for 5 minutes each, then sequentially in 95%, 90%, 80%, 70%, and 50% ethanol for 5 minutes each. Afterwards, to completely remove paraffin, immerse it in 1X Target retrieval solution, boil for 20 minutes, and then cool at RT for about 30 minutes. After washing, mark the boundaries of the tissue, add peroxidase, and let the tissue rest in a humidified chamber filled with water for 20 minutes. After washing, block, wash again, attach antibody (Table 4) and rest overnight at 4°C. After washing, remove the moisture, attach the secondary antibody, and rest in a humidified chamber filled with water for 1 hour and 30 minutes. After washing, remove the moisture. Drop DAB solution on the tissue, briefly stained in a humidified chamber, and observe under a microscope. After checking the staining intensity, counterstain with Hematoxylin and observe under a microscope.

15. Statistical analysis

The results are presented as mean values accompanied by their respective standard deviations. Each experimental procedure was repeated a minimum of three times to ensure reliability and consistency. Statistical analyses were conducted using two-tailed Student's t-tests to assess the significance of the

observed differences between groups. A significance level of $P < 0.05$ was adopted as the threshold for determining statistical significance, enhancing the rigor and robustness of the analysis.

RESULTS

1. S100A11 expression is upregulated in breast cancer tissues

The identification and characterization of DEGs make important contributions to our understanding of the molecular mechanisms underlying diseases [34, 35]. Consequently, in this study, I sought to use DEGs to search for specific biomarkers associated with breast cancer. Accordingly, I performed GEO2R analysis on the GSE32641 dataset and identified 2,422 significantly upregulated DEGs. On the basis of analysis using standard threshold values ($P < 0.001$, logFC > 2.0), 1,246 genes were selected, among which, S100A11 was the most significantly upregulated gene (Figure 1A). To determine the clinical significance of S100A11 in the progression of breast cancer, I used the GEPIA database. The evaluation of S100A11 expression levels in normal and cancer tissues revealed that the mRNA expression of S100A11 was elevated in breast cancer tissues compared with normal tissues (Figure 1B). To verify these results, tumor tissue from actual patients with breast cancer collected at Asan Medical Center in Seoul and adjacent normal tissue were used to verify S100A11 protein expression. The results demonstrated that S100A11 protein expression was higher in cancer tissues compared to normal tissues (Figure 1C). Subsequently, immunohistochemistry analysis was conducted on clinical tissue samples to determine whether S100A11 expression correlated with the grade of patients with breast cancer. Results demonstrated that S100A11 expression was increased in both the nucleus and cytoplasm of cancer tissues depending on the grade, in contrast to the low expression observed in normal tissues (Figure 1D). Examining the correlation between S100A11 expression and patient prognosis revealed that patients with breast cancer high expression of S100A11 had reduced overall survival (Figure 1E), indicating that S100A11 could serve as a biomarker for breast cancer. Moreover, given that the expression of S100A11 is closely associated with patient prognosis, this highlights the potential importance of the S100A11 protein as a therapeutic target.

2. S100A11 knockdown causes cell death in TNBC

To further investigate the role of S100A11 in breast cancer progression, I determined the mRNA and protein levels of S100A11 in different breast cancer cell lines. In all assessed cell lines, the expression of S100A11 was consistently upregulated (Figure 2A). To determine the functional effects of S100A11 on breast cancer, I performed S100A11 knockdown in breast cancer cell lines, which had the effect of promoting cell death in all assessed lines, particularly in TNBC cell lines. These observations would indicate that S100A11 has a selective effect on TNBC cells (Figure 2B). To investigate the relationship between TNBC and S100A11, a volcano plot was created using GSE data. As a result, S100A11 was

significantly upregulated in tissues of patients with TNBC compared to tissues of patients with non-TNBC (Supplementary Figure 1A). In this context, Caspase 3 and Cytochrome c, established markers of apoptosis, have been demonstrated to play central roles in the cleavage of different cell substrates [36, 37]. Additionally, Caspase 8 has been identified as a representative protein of apoptosis mediated via an extrinsic pathway [38, 39]. Accordingly, to elucidate the mechanisms by which the knockdown of S100A11 promotes apoptosis, I examined the expression of Cleaved caspase 3, Cytochrome c, and Cleaved caspase 8 in TNBC cell lines. Western blot analysis revealed a significant increase in the expression of Cleaved caspase 3 and Cytochrome c; Cleaved caspase 8 expression remained unchanged under these conditions (Figure 2C). Knockdown of S100A11 did not change the expression of Cleaved caspase 3, Cytochrome c, and Cleaved caspase 8 in MCF-7 cells, a representative ER-positive cell line (Supplementary Figure 1B). This suggests that cell death induced by the S100A11 knockdown is mediated via an intrinsic pathway.

3. S100A11 *inhibition promotes apoptosis in TNBC*

To further verify the apoptotic effects of S100A11, I performed S100A11 knockdown again and thereafter confirmed apoptosis based on Annexin V/PI staining, a routine method for verifying apoptosis [40]. A significant induction of apoptosis was indeed detected in all cell lines in which the expression of S100A11 had been inhibited, increasing from 11.6 to 71.2%, 8.8 to 86.8%, and 12.0 to 71.0% in the HCC-1395, HCC-1937, and MDA-MB-231 cell lines, respectively (Figure 3A). In addition, cell cycle analysis was performed to determine the proportion of cells at the sub-G1 stage, which is indicative of apoptotic cells [41]. Subsequent observations revealed clear increases in the proportions of sub-G1 phase cells in all cells lines following S100A11 knockdown, with increases from 3.2 to 32.9%, 2.0 to 54.6%, and 4.0 to 30.1% in the HCC-1395, HCC-1937, and MDA-MB-231 cell lines, respectively (Figure 3B). To further verify apoptosis, I performed TUNEL analysis, a method used to detect DNA fragmentation, which is a hallmark of apoptosis [42]. DNA fragmentation was indeed detected in all cell lines with S100A11 knockdown, as revealed by green FITC staining (Figure 3C, D). Collectively, these findings provide convincing evidence to indicate that the inhibition of S100A11 expression induces apoptosis in TNBC cell lines.

4. S100A11 *knockdown induces BIM-dependent apoptosis in TNBC*

Having successfully confirmed the induction of apoptosis by S100A11 knockdown, I subsequently sought to identify the genes associated with the apoptotic process. In this regard, the BH3-only group of proteins has long been known to play essential roles in apoptosis [43, 44]. Close examination of the BH3-only proteins expression profiles revealed significantly higher BIM levels, unlike the other genes

examined (Figure 4A). In the MCF-7 cells, knockdown of S100A11 did not change the expression of BIM (Supplementary Figure 2A). I then used quantitative real-time PCR to closely examine the regulatory impact of S100A11 on BIM at the transcriptional level and clearly established a significant BIM upregulation, in stark contrast to the other genes examined (Figure 4B). Simultaneous knockdown of S100A11 and BIM to establish the causal relationship between S100A11 and BIM-mediated cell death (Figure 4C) revealed a significant reduction in the apoptosis of cells that received the co-knockdown treatment compared with that with S100A11 knockdown alone (Figure 4D). These observations accordingly provided evidence to indicate that the apoptosis induced by inhibition of S100A11 is mediated via a regulation of BIM.

5. Depletion of **S100A11** *activates the nuclear translocation of FoxO3a*

To gain further insights on the specific pathway of BIM-mediated cell death induced by the inhibition of S100A11, I examined the expression of proteins known to be closely associated with BIM, namely, phosphorylated AKT (p-AKT), phosphorylated ERK1/2 (p-ERK1/2) [45, 46]. Among them, only p-AKT showed any appreciable changes in expression (Figure 5A). According to reported studies, FoxO3a has been identified as a representative transcription factor that regulates the expression of BIM [47], and shown that when phosphorylated by p-AKT, FoxO3a is unable to enter the nuclear, and is subsequently degraded in the cytoplasm [48, 49]. Based on these findings, I hypothesized that the low apoptosis observed in TNBC is attributable to the fact that S100A11 enhances AKT phosphorylation, thereby preventing the FoxO3a-mediated transcription of BIM. As a result of checking the expression changes of representative proteins related to the transcription of BIM, there were no changes in the expression of other proteins except for FoxO3a (Supplementary Figure 3A). As shown in Figure 5B, in response to S100A11 knockdown, there was a reduction in the levels of phosphorylated FoxO3a (p-FoxO3a) and a corresponding increase in those of FoxO3a. To confirm whether this response is associated with FoxO3a localization, cell nucleus and cytoplasm were separated and observed, and it was verified that FoxO3a moved to the nuclear due to S100A11 knockdown (Figure 5C). To verify the previous results once again, immunofluorescence analysis using fluorescent dye-labeled antibodies was performed. In cell lines with S100A11 (shown in red) knockdown, FoxO3a (shown in green) can be seen distributed in the nucleus (Figure 5D). Collectively, these findings indicate that in response to the inhibition of S100A11, FoxO3a remains in a non-phosphorylated state and thereby undergoes localization to the nucleus, wherein it transcribes BIM.

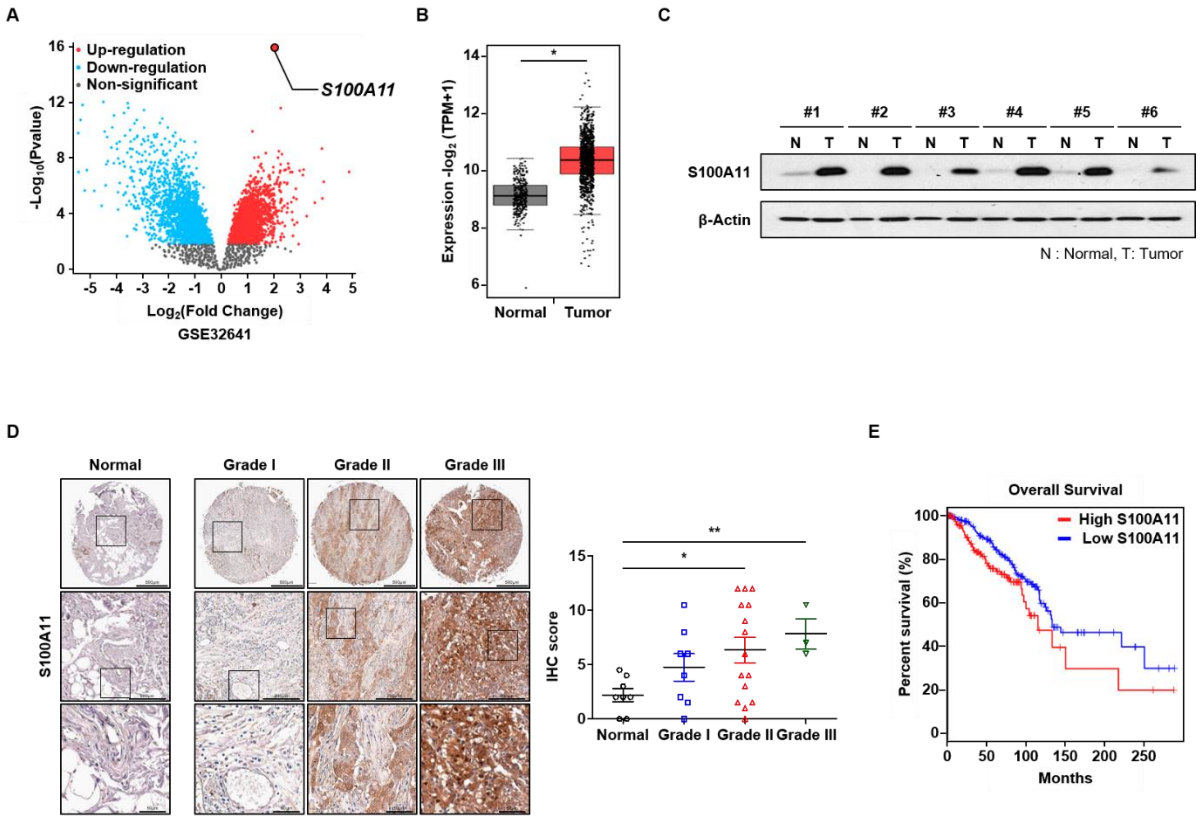

Figure 1. The upregulated expression of S100A11 in patients with breast cancer. (A) A volcano plot of differentially expressed genes identified in the GSE32641 dataset. (B) Expression profile of S100A11 based on the GEPIA database. (C) The expression of S100A11 in the tissues of patients with breast cancer. (D) A tissue microarray containing breast cancer specimens stained for S100A11. Representative images and quantification of each tumor grade. Scale bar: 500, 200, and 50 μm. (E) The overall survival of patients with low (Blue) or high (Red) expression of the S100A11 protein. $P = 0.0017$, P(HR) = 0.0019. *, $P < 0.05$ and **, $P < 0.01$ indicate statistically significant differences from values obtained for the control group.

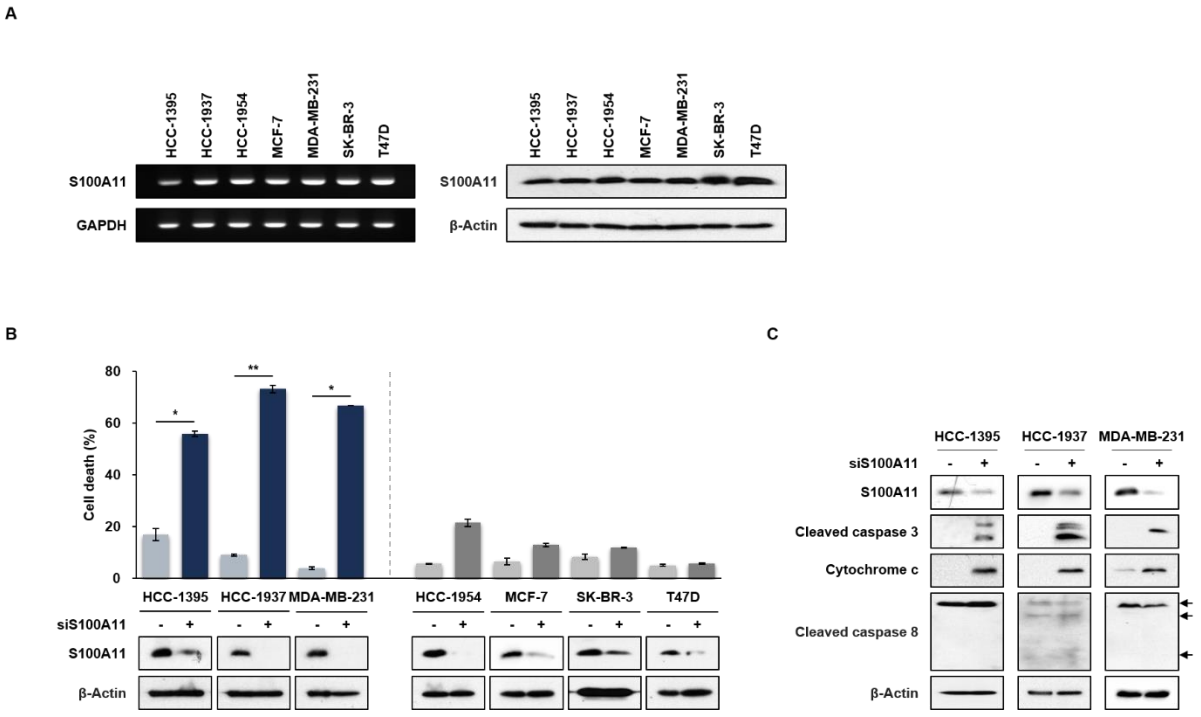

Figure 2. The inhibition of S100A11 promotes cell death. (A) Determination of S100A11 mRNA and protein levels in different breast cancer cell lines. (B) Cell death following inhibition of S100A11. (C) Western blot assay of apoptotic protein expression following S100A11 inhibition. *, $P < 0.05$ and **, $P < 0.01$ indicate statistically significant differences from values obtained for the control group.

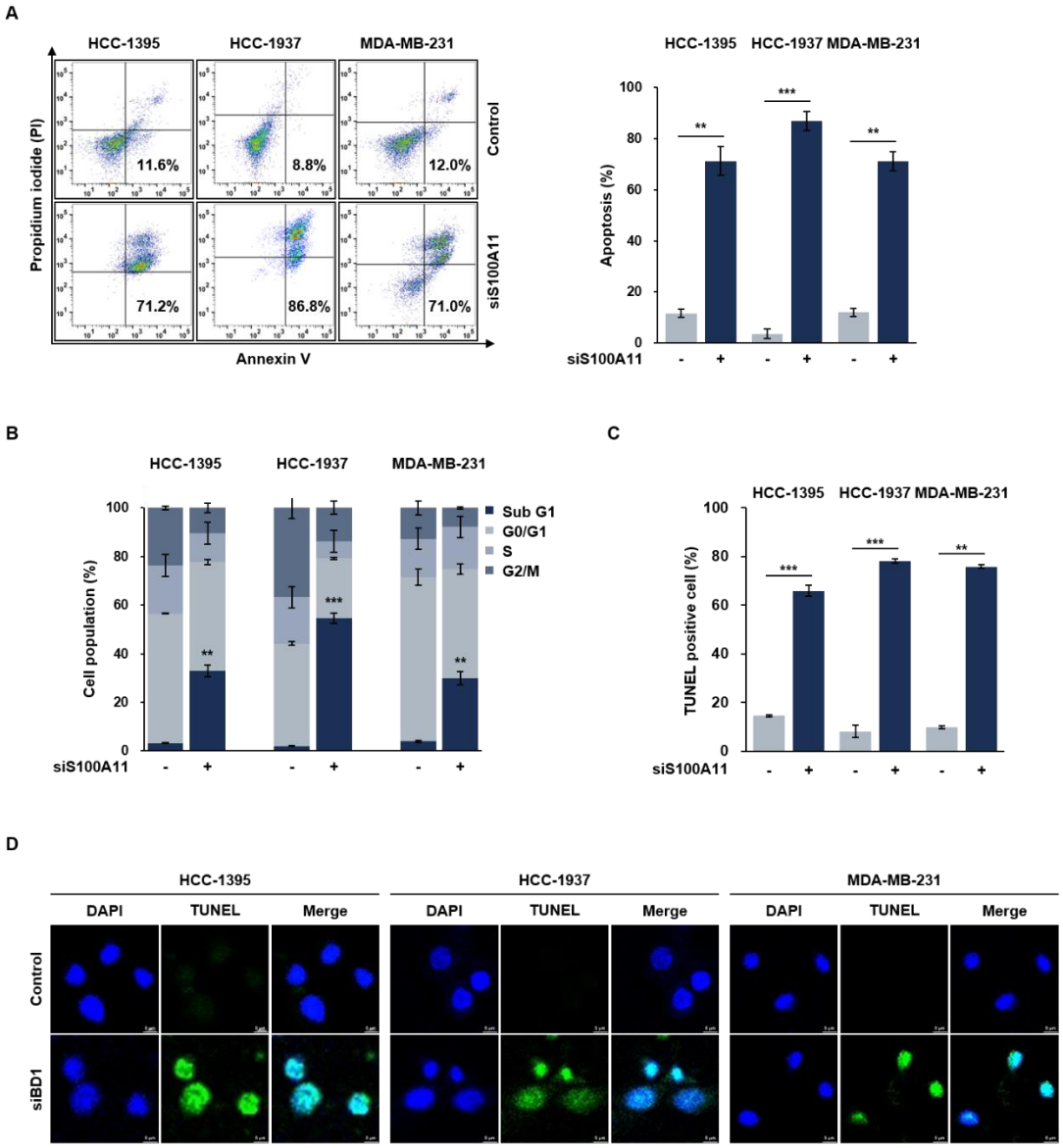

Figure 3. Knockdown of S100A11 promotes apoptosis in TNBC. (A) Annexin V/PI staining in TNBC cell lines. (B) Cell cycle analysis showing significantly increased sub-G1 arrest in TNBC cell lines. (C) The statistical analysis results for the percentage of TUNEL-positive cells normalized to the control group. (D) Representative images of the apoptotic ratio of cells following S100A11 knockdown analyzed using a TUNEL assay. Scale bar: 5 μm. **, $P < 0.01$ and ***, $P < 0.001$ indicate statistically significant differences from values obtained for the control group.

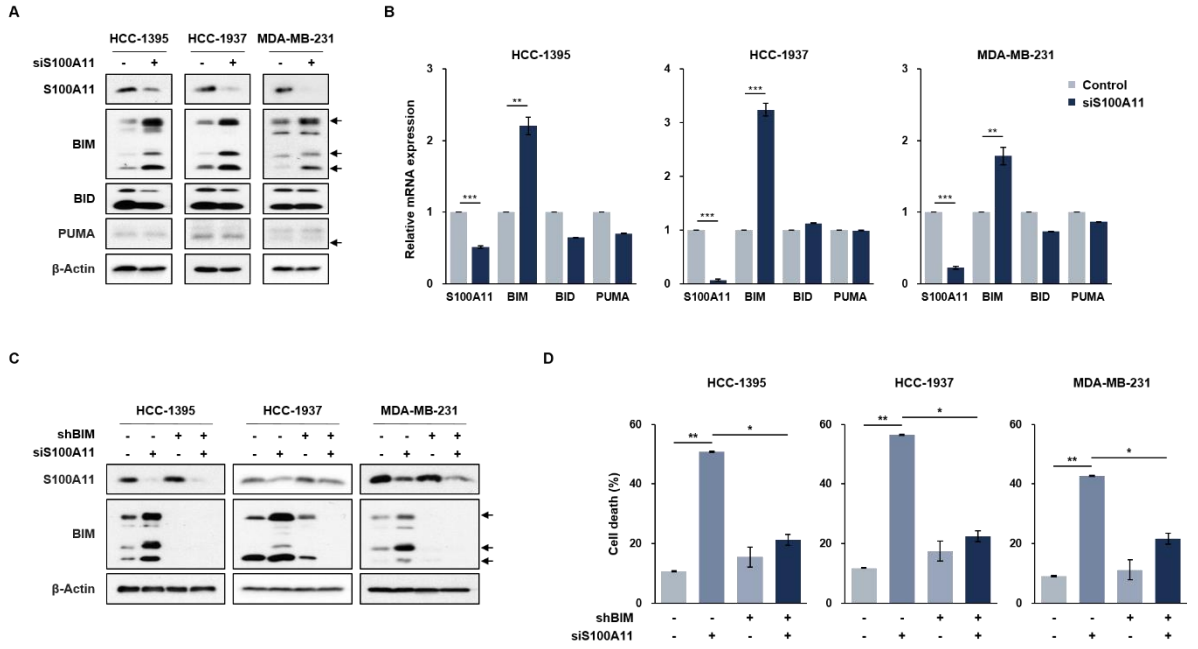

Figure 4. Suppression of S100A11 promotes an increase in BIM-dependent apoptosis. (A) Protein expression of apoptosis-associated genes in TNBC cells following S100A11 knockdown. (B) mRNA expression of BH3-only proteins in TNBC cell lines upon S100A11 knockdown. (C) Effect of co-transfection with siS100A11 and shBIM on TNBC cell lines. (D) Cell death induced by co-transfection in TNBC cell lines. *, $P < 0.05$, **, $P < 0.01$, and ***, $P < 0.001$ indicate statistically significant differences from values obtained for the control group.

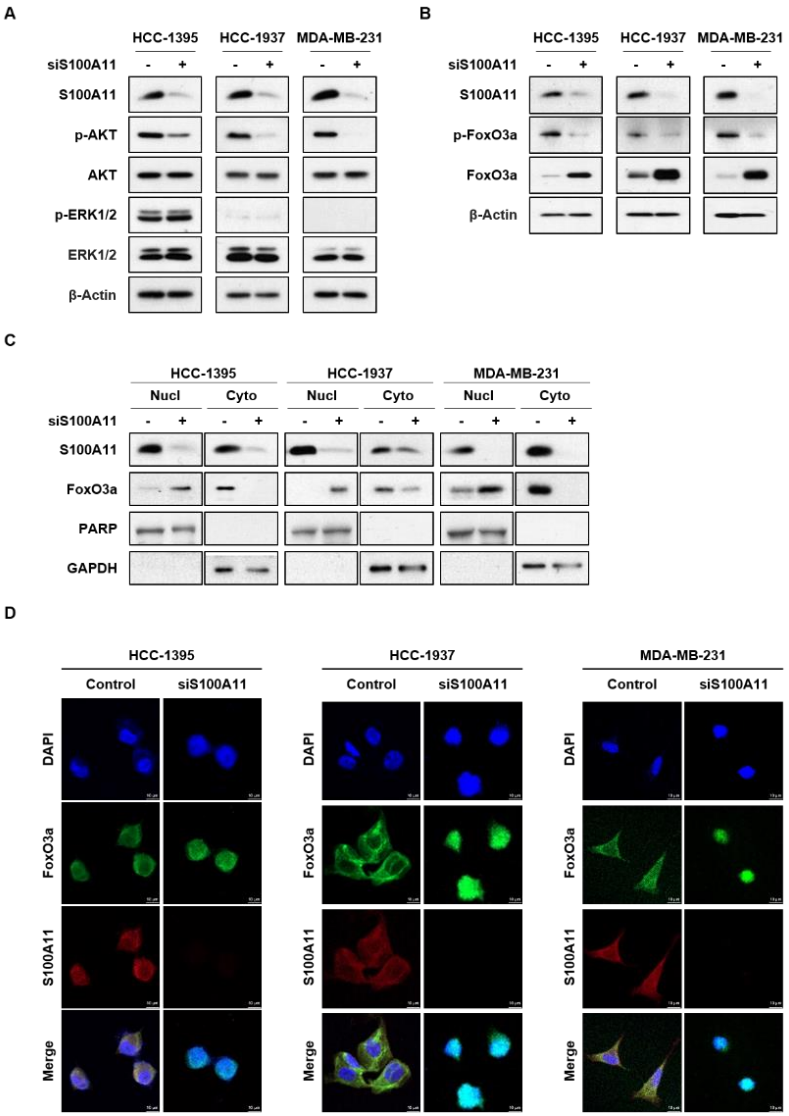

Figure 5. Inhibition of S100A11 induces the nuclear translocation of FoxO3a. (A) Analysis of the pathways regulated by S100A11 in TNBC cell lines. (B) Changes in FoxO3a expression in TNBC cell lines. (C) Western blot assay of subcellular fractions from TNBC cells following S100A11 knockdown. (D) Immunofluorescence assay to observe nuclear translocation of FoxO3a in TNBC cell lines. Scale bar: 5 μm.

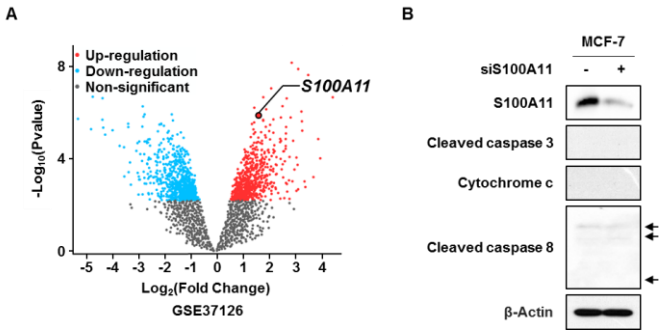

Supplementary Figure 1. (A) Increased expression of S100A11 in tissues from patients with TNBC. (B) Western blot assay of apoptotic protein expression in the ER-positive MCF-7 cell line following S100A11 inhibition.

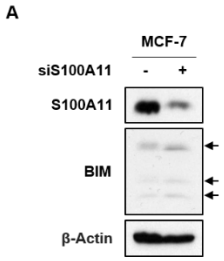

Supplementary Figure 2. (A) Protein expression of BIM in ER-positive MCF-7 cell line following S100A11 inhibition.

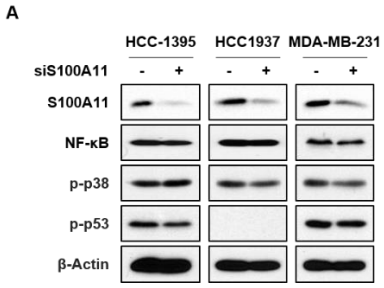

Supplementary Figure 3. (A) After S100A11 knockdown, NF-κB, p-p38, and p-p53 expression was analyzed by Western blot.

Table 1. List of PCR primer sequences.

Gene		Primer sequences (5' – 3')
S100A11	Sense	ATG GCA AAA ATC TCC AGC CC
	Anti-sense	TCA GGT CCG CTT CTG GGA
BIM	Sense	CAA GAG TTG CGG CGT ATT GGA G
	Anti-sense	ACA CCA GGC GGA CAA TGT AAC G
BID	Sense	TGA GGT CAA CAA CGG TTC CA
	Anti-sense	GGA AGC CAA ACA CCA GTA GGT T
PUMA	Sense	CCT GGA GGG TCC TGT ACA ATC T
	Anti-sense	TCT GTG GCC CCT GGG TAA G
GAPDH	Sense	GTG ATG GGA TTT CCA TTG AT
	Anti-sense	GGA GTC AAC GGA TTT GGT

Table 2. List of western blot assay antibodies.

Protein	Company	Cat. No.
Calgizzarin (S100A11)	Santa Cruz Biotechnology	sc-390250
Cleaved Caspase-3	Cell Signaling Technology	9664s
Caspase 8	Cell Signaling Technology	9746s
Cytochrome c	Cell Signaling Technology	4272s
BIM	Cell Signaling Technology	2819
BID	Cell Signaling Technology	2002s
p38 MAPK	Cell Signaling Technology	9212s
NFκB p65 (F-6)	Santa Cruz Biotechnology	sc-8008
PUMA	Cell Signaling Technology	4976s
p-AKT	Cell Signaling Technology	4060s
p44/42 MARK (Erk1/2)	Cell Signaling Technology	4695s
p-p53	Cell Signaling Technology	9284s
p-FoxO3a	Cell Signaling Technology	9466s
FoxO3a	Cell Signaling Technology	12829S
β-Actin	Santa Cruz Biotechnology	sc-47778

Table 3. List of immunofluorescence assay antibodies.

Protein	Company	Cat. No.
Calgizzarin (S100A11)	Santa Cruz Biotechnology	sc-390250
FoxO3a	Cell Signaling Technology	12829S

Table 4. List of immunohistochemistry assay antibody.

Protein	Company	Cat. No.
Calgizzarin (S100A11)	Santa Cruz Biotechnology	sc-390250

DISCUSSION

Breast cancer is the leading cause of cancer-related deaths in the female population and is diagnosed extensively worldwide [50–52]. Unlike other subtypes of this cancer, TNBC is characterized by particularly rapid cell growth and is highly invasive. The average survival period post-diagnosis is approximately 2 years, indicating the poor survival rate compared with that of patients with general breast cancer [53]. Although several treatments are being developed for breast cancer, developing such treatments for TNBC negative for ER, PR, and HER2 has proved particularly challenging, given that tumors do not respond to drugs targeting these receptors [54]. This accordingly highlights the necessity of developing effective treatments of TNBC. Currently, the FDA-approved treatments for TNBC include PARP inhibitors (Lynparza and Talzenna), anthracyclines (Doxorubicin, Epirubicin), taxane-based chemotherapy (Paclitaxel, Docetaxel), and ADC (Sacituzumab govitecan) [55]. However, these drugs tend to be non-specific and have been associated with fatal side effects.

On the basis of GEO data analysis, I established that the S100A11 protein is significantly upregulated in the tissues of patients with breast cancer (Figure 1A), and with reference to the TCGA database, I found that the mRNA expression of S100A11 is elevated in breast cancer (Figure 1B). By performing western blotting, I demonstrated that S100A11 is highly expressed in breast cancer tissues, and immunohistochemistry analysis revealed that S100A11 expression is correlated with breast cancer grade (Figure 1C, D). High expression of S100A11 was also found to be associated with patient prognosis (Figure 1E). On the basis of these findings, I hypothesized that S100A11 could serve as a biomarker for patients with breast cancer and that it has potential application as a target for the treatment of breast cancer.

Initially, to clarify the function of S100A11 in breast cancer, I examined the elevated expression of this protein in different breast cancer cell lines (Figure 2A), and thereby confirmed that cell death is induced in response to an inhibition of S100A11, and that this effect is more pronounced in TNBC cell lines (Figure 2B). This cell death was confirmed to be apoptotic based on observed increases in the levels of Cleaved caspase 3 and the secretion of Cytochrome c (Figure 2C). These findings accordingly provided evidence to indicate that S100A11 play an important role in cell survival in TNBC. To further confirm that apoptosis is indeed induced in response to the inhibition of S100A11, I examined apoptosis using several methodological approaches (Figure 3A–C). Established this apoptotic response, I subsequently investigated the mechanisms whereby S100A11 influences cell survival in TNBC. Knockdown of S100A11 was found to promote increases in the expression of BIM, a BH3-only protein (Figure 4A, B). Furthermore, co-transfection of cells with siS100A11 and shBIM was found to restore apoptosis, based on which, I demonstrated that BIM functions as a key factor inducing apoptosis after

inhibition of S100A11 (Figure 4C, D). In this regard, it has previously been reported that FoxO3a is phosphorylated and degraded by p-AKT, and when not phosphorylated, binds to the promoter of BIM, and thereby transcribes this protein [56, 57]. In response to the knockdown of S100A11, there was an increase in the expression of BIM at the transcriptional level, thereby confirming the expression of the associated pathway, including AKT and the known transcription factor FoxO3a (Figure 5A, B). Given that the interaction between FoxO3a and BIM is dependent on subcellular localization, I isolated nuclear and cytoplasmic fractions to determine the localization of FoxO3a in cells following S100A11 knockdown, which accordingly revealed that the inhibition of S100A11 is associated with the nuclear translocation of FoxO3a (Figure 5C, D). Collectively, these findings indicate that S100A11 contributes to cell survival by regulating the expression of AKT, FoxO3a, and BIM.

To the best of my knowledge, this is the first study to investigate the cellular function of S100A11 in the context of breast cancer, and specifically TNBC. S100A11 was established to be highly expressed in TNBC and appears to regulate cell growth via the AKT/FoxO3a/BIM signaling pathway.

CONCLUSION

In this study, the expression of S100A11 was established to be upregulated in breast cancer tissues, and the knockdown of this protein was found to induce cell death in breast cancer cell lines, particularly in TNBC cell lines. Moreover, this cell death was shown to be attributable to apoptosis. In addition, evidence indicates that the effects induced by the inhibition of S100A11 are mediated via regulation of the AKT/FoxO3a/BIM signaling pathway.

On the basis of the findings of this study, I propose S100A11 as a novel biomarker and therapeutic target for the treatment of patients with TNBC. Given the complex characteristics of the TNBC subtype, and a current lack of research on biomarkers for the targeted treatment of Triple negative breast cancer, further research is necessary to identify effective treatments for this particularly aggressive cancer subtype.

REFERENCES

1. Ye, F., Dewanjee, S., Li, Y., Jha, N. K., Chen, Z. S., Kumar, A., ... & Tang, H. (2023). Advancements in clinical aspects of targeted therapy and immunotherapy in breast cancer. Molecular cancer, 22(1), 105.

2. Newman, L. (2023). Oncologic anthropology: Global variations in breast cancer risk, biology, and outcome. Journal of Surgical Oncology, 128(6), 959-966.

3. Arnold, M., Morgan, E., Rumgay, H., Mafra, A., Singh, D., Laversanne, M., ... & Soerjomataram, I. (2022). Current and future burden of breast cancer: Global statistics for 2020 and 2040. The Breast, 66, 15-23.

4. Fox, S., Speirs, V., & Shaaban, A. M. (2022). Male breast cancer: an update. Virchows Archiv, 480(1), 85-93.

5. Arnold, M., Morgan, E., Rumgay, H., Mafra, A., Singh, D., Laversanne, M., ... & Soerjomataram, I. (2022). Current and future burden of breast cancer: Global statistics for 2020 and 2040. The Breast, 66, 15-23.

6. Yin, L., Duan, J. J., Bian, X. W., & Yu, S. C. (2020). Triple-negative breast cancer molecular subtyping and treatment progress. Breast Cancer Research, 22, 1-13.

7. Dai, X., Chen, A., & Bai, Z. (2014). Integrative investigation on breast cancer in ER, PR and HER2-defined subgroups using mRNA and miRNA expression profiling. Scientific reports, 4(1), 6566.

8. Aysola, K., Desai, A., Welch, C., Xu, J., Qin, Y., Reddy, V., ... & Rao, V. N. (2013). Triple negative breast cancer–an overview. Hereditary genetics: current research, 2013(Suppl 2).

9. Yin, L., Duan, J. J., Bian, X. W., & Yu, S. C. (2020). Triple-negative breast cancer molecular subtyping and treatment progress. Breast Cancer Research, 22, 1-13.

10. Cai, S. L., Liu, J. J., Liu, Y. X., Yu, S. H., Liu, X., Lin, X. Q., ... & Zhang, J. (2023). Characteristics of recurrence, predictors for relapse and prognosis of rapid relapse triple-negative breast cancer. Frontiers in Oncology, 13, 1119611.

11. Sedaghat, F., & Notopoulos, A. (2008). S100 protein family and its application in clinical practice. Hippokratia, 12(4), 198.

12. Zimmer, D. B., Eubanks, J. O., Ramakrishnan, D., & Criscitiello, M. F. (2013). Evolution of the S100 family of calcium sensor proteins. Cell calcium, 53(3), 170-179.

13. Gross, S. R., Sin, C. G. T., Barraclough, R., & Rudland, P. S. (2014). Joining S100 proteins and migration: for better or for worse, in sickness and in health. Cellular and molecular life sciences, 71, 1551-1579.

14. Marenholz, I., Heizmann, C. W., & Fritz, G. (2004). S100 proteins in mouse and man: from evolution to function and pathology (including an update of the nomenclature). Biochemical and biophysical research communications, 322(4), 1111-1122.

15. Bresnick, A. R., Weber, D. J., & Zimmer, D. B. (2015). S100 proteins in cancer. Nature Reviews Cancer, 15(2), 96-109.

16. Ghavami, S., Eshragi, M., Ande, S. R., Chazin, W. J., Klonisch, T., Halayko, A. J., ... & Los, M. (2010). S100A8/A9 induces autophagy and apoptosis via ROS-mediated cross-talk between mitochondria and lysosomes that involves BNIP3. Cell research, 20(3), 314-331.

17. Xia, C., Braunstein, Z., Toomey, A. C., Zhong, J., & Rao, X. (2018). S100 proteins as an important regulator of macrophage inflammation. Frontiers in immunology, 8, 1908.

18. Singh, P., & Ali, S. A. (2022). Multifunctional role of S100 protein family in the immune system: An update. Cells, 11(15), 2274.

19. Sattar, Z., Lora, A., Jundi, B., Railwah, C., & Geraghty, P. (2021). The S100 protein family as players and therapeutic targets in pulmonary diseases. Pulmonary Medicine, 2021.

20. Zhang, L., Zhu, T., Miao, H., & Liang, B. (2021). The calcium binding protein S100A11 and its roles in diseases. Frontiers in cell and developmental biology, 9, 693262.

21. Memon, A. A., Sorensen, B. S., Meldgaard, P., Fokdal, L., Thykjaer, T., & Nexo, E. (2005). Down-regulation of S100C is associated with bladder cancer progression and poor survival. Clinical cancer research, 11(2), 606-611.

22. Niu, Y., Shao, Z., Wang, H., Yang, J., Zhang, F., Luo, Y., ... & Zhao, L. (2016). LASP1-S100A11 axis promotes colorectal cancer aggressiveness by modulating TGFβ/Smad signaling. Scientific Reports, 6(1), 26112.

23. Li, W., Han, F., Tang, K., Ding, C., Xiong, F., Xiao, Y., ... & Gao, H. (2023). Inhibiting NF-κB-S100A11 signaling and targeting S100A11 for anticancer effects of demethylzeylasteral in human colon cancer. Biomedicine & Pharmacotherapy, 168, 115725.

24. Koh, S. A., & Lee, K. H. (2018). HGF-mediated S100A11 overexpression enhances proliferation and invasion of gastric cancer. American Journal of Translational Research, 10(11), 3385.

25. Cui, Y., Li, L., Li, Z., Yin, J., Lane, J., Ji, J., & Jiang, W. G. (2021). Dual effects of targeting S100A11

on suppressing cellular metastatic properties and sensitizing drug response in gastric cancer. Cancer cell international, 21(1), 243.

26. Zheng, M., Meng, H., Li, Y., Shi, J., Han, Y., Zhao, C., ... & Wang, Y. (2023). S100A11 Promotes Metastasis via AKT and ERK Signaling Pathways and Has a Diagnostic Role in Hepatocellular Carcinoma. International Journal of Medical Sciences, 20(3), 318.

27. Hao, J., Wang, K., Yue, Y., Tian, T., Xu, A., Hao, J., ... & He, D. (2012). Selective expression of S100A11 in lung cancer and its role in regulating proliferation of adenocarcinomas cells. Molecular and cellular biochemistry, 359, 323-332.

28. Liu, Y., Han, X., & Gao, B. (2015). Knockdown of S100A11 expression suppresses ovarian cancer cell growth and invasion. Experimental and Therapeutic Medicine, 9(4), 1460-1464.

29. Xiao, M., Li, T., Ji, Y., Jiang, F., Ni, W., Zhu, J., ... & Ni, R. (2018). S100A11 promotes human pancreatic cancer PANC-1 cell proliferation and is involved in the PI3K/AKT signaling pathway. Oncology letters, 15(1), 175-182.

30. Ji, Y. F., Li, T., Jiang, F., Ni, W. K., Guan, C. Q., Liu, Z. X., ... & Xiao, M. B. (2019). Correlation between S100A11 and the TGF-β 1/SMAD4 pathway and its effects on the proliferation and apoptosis of pancreatic cancer cell line PANC-1. Molecular and Cellular Biochemistry, 450, 53-64.

31. Han, D., Guo, C., Cheng, H., Lu, J., Hou, Z., Zhang, X., ... & Shang, P. (2024). Downregulation of S100A11 promotes T cell infiltration by regulating cancer-associated fibroblasts in prostate cancer. International Immunopharmacology, 111323.

32. Liu, L., Miao, L., Liu, Y., Qi, A., Xie, P., Chen, J., & Zhu, H. (2017). S100A11 regulates renal carcinoma cell proliferation, invasion, and migration via the EGFR/Akt signaling pathway and E-cadherin. Tumor Biology, 39(5), 1010428317705337.

33. Tang, Z., Kang, B., Li, C., Chen, T., & Zhang, Z. (2019). GEPIA2: an enhanced web server for large-scale expression profiling and interactive analysis. Nucleic acids research, 47(W1), W556-W560.

34. Rodriguez-Esteban, R., & Jiang, X. (2017). Differential gene expression in disease: a comparison between high-throughput studies and the literature. BMC medical genomics, 10, 1-10.

35. Porcu, E., Sadler, M. C., Lepik, K., Auwerx, C., Wood, A. R., Weihs, A., ... & Kutalik, Z. (2021). Differentially expressed genes reflect disease-induced rather than disease-causing changes in the transcriptome. Nature Communications, 12(1), 5647.

36. Chang, H. Y., & Yang, X. (2000). Proteases for cell suicide: functions and regulation of caspases. Microbiology and molecular biology reviews, 64(4), 821-846.

37. Li, P., Zhou, L., Zhao, T., Liu, X., Zhang, P., Liu, Y., ... & Li, Q. (2017). Caspase-9: structure, mechanisms and clinical application. Oncotarget, 8(14), 23996

38. Tummers, B., & Green, D. R. (2017). Caspase-8: regulating life and death. Immunological reviews, 277(1), 76-89.

39. Kominami, K., Nakabayashi, J., Nagai, T., Tsujimura, Y., Chiba, K., Kimura, H., ... & Sakamaki, K. (2012). The molecular mechanism of apoptosis upon caspase-8 activation: quantitative experimental validation of a mathematical model. Biochimica et Biophysica Acta (BBA)-Molecular Cell Research, 1823(10), 1825-1840.

40. Vermes, I., Haanen, C., Steffens-Nakken, H., & Reutellingsperger, C. (1995). A novel assay for apoptosis flow cytometric detection of phosphatidylserine expression on early apoptotic cells using fluorescein labelled annexin V. Journal of immunological methods, 184(1), 39-51.

41. Riccardi, C., & Nicoletti, I. (2006). Analysis of apoptosis by propidium iodide staining and flow cytometry. Nature protocols, 1(3), 1458-1461.

42. Kyrylkova, K., Kyryachenko, S., Leid, M., & Kioussi, C. (2012). Detection of apoptosis by TUNEL assay. Odontogenesis: Methods and Protocols, 41-47.

43. Giam, M., Huang, D. C. S., & Bouillet, P. (2008). BH3-only proteins and their roles in programmed cell death. Oncogene, 27(1), S128-S136.

44. Huang, D. C., & Strasser, A. (2000). BH3-only proteins—essential initiators of apoptotic cell death. Cell, 103(6), 839-842.

45. Luciano, F., Jacquel, A., Colosetti, P., Herrant, M., Cagnol, S., & Auberger, P. (2003). Phosphorylation of Bim-EL by Erk1/2 on serine 69 promotes its degradation via the proteasome pathway and regulates its proapoptotic function. Oncogene, 22(43), 6785-6793.

46. Yuan, Y., Long, H., Zhou, Z., Fu, Y., & Jiang, B. (2023). PI3K–AKT-Targeting breast cancer treatments: Natural products and synthetic compounds. Biomolecules, 13(1), 93.

47. Sunters, A., de Mattos, S. F., Stahl, M., Brosens, J. J., Zoumpoulidou, G., Saunders, C. A., ... & Lam, E. W. F. (2003). FoxO3a transcriptional regulation of Bim controls apoptosis in paclitaxel-treated breast cancer cell lines. Journal of Biological Chemistry, 278(50), 49795-49805.

48. Sun, B., Chen, H., Wang, X., & Chen, T. (2023). Regorafenib induces Bim-mediated intrinsic apoptosis by blocking AKT-mediated FOXO3a nuclear export. Cell Death Discovery, 9(1), 37.

49. Taylor, S., Lam, M., Pararasa, C., Brown, J. E., Carmichael, A. R., & Griffiths, H. R. (2015). Evaluating the evidence for targeting FOXO3a in breast cancer: a systematic review. Cancer cell

international, 15, 1-9.

50. Wilkinson, L., & Gathani, T. (2022). Understanding breast cancer as a global health concern. The British Journal of Radiology, 95(1130), 20211033.

51. Łukasiewicz, S., Czeczelewski, M., Forma, A., Baj, J., Sitarz, R., & Stanisławek, A. (2021). Breast cancer—epidemiology, risk factors, classification, prognostic markers, and current treatment strategies—an updated review. Cancers, 13(17), 4287.

52. Azamjah, N., Soltan-Zadeh, Y., & Zayeri, F. (2019). Global trend of breast cancer mortality rate: a 25-year study. Asian Pacific journal of cancer prevention: APJCP, 20(7), 2015.

53. Li, X., Yang, J., Peng, L., Sahin, A. A., Huo, L., Ward, K. C., ... & Meisel, J. L. (2017). Triple-negative breast cancer has worse overall survival and cause-specific survival than non-triple-negative breast cancer. Breast cancer research and treatment, 161, 279-287.

54. Deepak, K. G. K., Vempati, R., Nagaraju, G. P., Dasari, V. R., Nagini, S., Rao, D. N., & Malla, R. R. (2020). Tumor microenvironment: Challenges and opportunities in targeting metastasis of triple negative breast cancer. Pharmacological research, 153, 104683.

55. Mandapati, A., & Lukong, K. E. (2023). Triple negative breast cancer: Approved treatment options and their mechanisms of action. Journal of cancer research and clinical oncology, 149(7), 3701-3719.

56. Song, J., Zhang, W., Wang, J., Yang, H., Zhou, Q., Wang, H., ... & Du, G. (2019). Inhibition of FOXO3a/BIM signaling pathway contributes to the protective effect of salvianolic acid A against cerebral ischemia/reperfusion injury. Acta Pharmaceutica Sinica B, 9(3), 505-515.

57. Wang, X. L., Wu, Y., Tan, L. B., Tian, Z., Liu, J. H., Zhu, D. S., & Zeng, S. M. (2012). Follicle-stimulating hormone regulates pro-apoptotic protein Bcl-2-interacting mediator of cell death-extra long (BimEL)-induced porcine granulosa cell apoptosis. Journal of Biological Chemistry, 287(13), 10166-10177.

국문 요약

유방암은 전 세계적으로 가장 많이 진단되는 암이다. 약 16%의 여성이 유방암에 걸리며, 이는 여성에서 암 관련 사망의 주요 원인이다. 다양한 아형을 특징으로 하는 유방암은 아형에 따라 치료법이 달라지기 때문에 아형의 분류가 매우 중요하다. 이를 분류하는 병리학적 지표로는 에스트로겐 수용체, 프로게스테론 수용체 및 인간 표피 성장 인자 수용체 2가 있다. 삼중음성유방암은 에스트로겐 수용체, 프로게스테론 수용체 및 인간 표피 성장 인자 수용체 2에 모두 음성인 유방암의 일종이다. 일반적으로 유방암의 발병률은 나이와 비례하지만, 삼중음성유방암 환자는 주로 40세 이하의 여성에게서 발병한다. 삼중음성유방암 환자는 전체 유방암 환자의 약 15–20%를 차지하며, 생존기간이 다른 유방암 아형을 가진 환자들에 비해 짧다. 매우 침습적이어서 원격 전이가 많이 발생하는데, 전이 후 평균 생존 기간은 13.3개월에 불과하다.

S100 칼슘 결합 단백질 A11 (*S100A11*)은 S100 계열의 S100A 단백질에 속하는 유전자로, 최근 여러 암 종에서 종양 억제 유전자 또는 종양 촉진 유전자로서 S100A11의 기능이 활발하게 보고되고 있다. GEO 데이터베이스를 사용하여 유방암 환자 및/또는 삼중음성유방암 환자의 정상 조직과 종양 조직을 비교하고 종양 조직에서 가장 유의하게 상향 조절된 S100A11을 동정하였다.

유방암 환자 조직을 통해 정상 조직 대비 종양 조직에서 S100A11의 발현이 상향 조절되는 것을 확인하였다. 이후 S100A11의 기능을 명확히 하기 위해 유방암 세포주에서 S100A11의 발현을 저해하였고, 그 결과 삼중음성유방암 세포주에서 높은 비율로 세포 사멸이 발생하였다. S100A11 저해 시 유도되는 세포 사멸은 다른 BH-3 only protein과 달리 BIM의 발현을 유의하게 증가시켰다. 세포 사멸이 BIM에 의해 발생되는 것인지를

확인하기 위해 S100A11과 BIM의 발현을 동시에 저해하였고, S100A11 억제로 유도된 세포 사멸이 감소하는 것을 확인하였다. 다음으로 S100A11을 저해한 후 BIM을 조절하는 여러 경로의 대표적인 단백질을 확인하였을 때, 인산화된 AKT의 발현만이 변화하는 것을 확인하였다. AKT 경로에 관여하는 BIM의 여러 전사 인자들을 확인한 결과, BIM의 프로모터에 결합한다고 알려진 FoxO3a의 발현만이 변화하였다. S100A11을 저해한 후, 세포 분획법과 면역 형광법 분석을 통해 FoxO3a의 위치가 세포질에서 핵 내로 전위되는 것을 확인하였다. 종합하자면, S100A11의 억제가 AKT/FoxO3a/BIM 신호 기전을 통해 삼중음성유방암 세포주에서 세포 사멸을 일으킴을 검증하였다.

결론적으로 본 연구에서는 유방암 환자에서 S100A11의 발현이 증가되어 있다는 것과 유방암 세포주에서 S100A11 억제에 따른 항암 효능 및 분자 기전을 검증하였다. 따라서, 이를 통해 삼중음성유방암의 새로운 바이오마커 및 치료 표적으로서 S100A11의 가능성을 제시하고자 한다.